JOURNAL OF SOLID STATE CHEMISTRY **100**, 151–159 (1992)

t-AlF_3: Crystal Structure Determination from X-Ray Powder Diffraction Data. A New MX_3 Corner-Sharing Octahedra 3D Network

A. LE BAIL AND J. L. FOURQUET

Laboratoire des Fluorures, U.R.A. C.N.R.S. 449, Faculté des Sciences, Université du Maine, 72017 Le Mans Cedex, France.

AND U. BENTRUP

Zentralinstitut für Anorganische Chemie, Rudower Chaussee 5., 0.1199 Berlin-Adlershof, Germany.

Received December 6, 1991; accepted March 13, 1992

t-AlF_3 is obtained from the thermolysis of $[(CH_3)_4N)]AlF_4 \cdot H_2O$ or amorphous $AlF_3 \cdot xH_2O$ ($x < 0.5$). The structure is determined from X-ray powder diffraction data by the direct methods and refined by the Rietveld method to $R_B = 0.024$, $R_P = 0.070$ and $R_{WP} = 0.097$. Space group *P4/nmm; a* = 10.1843 Å, *c* = 7.1738 Å; *Z* = 16. t-AlF_3 belongs to the family of 3D corner-sharing octahedra networks, the Al atoms lying at the points of a 3D six-connected net. A relation with $Na_4Ca_4Al_7F_{33}$ is found which may be considered as a stuffed polytype. © 1992 Academic Press, Inc.

Introduction

The finding of new geometries corresponding to simple stoichiometries becomes increasingly rare and should be emphasized. We present here a new MX_3 corner sharing octahedra tridimensional network adopted by t-AlF_3 (t for tetragonal).

When restricting consideration to the MX_3 stoichiometry, among the various families of structures, there is one where each M atom is connected to six others (through X atoms) so that the M atoms lie at the points of a 3D six-connected net. The simplest of such structures corresponds, in its most symmetrical configuration, to the primitive cubic lattice and represents the structure of crystalline ReO_3. All the main structure-types belonging to this family can be found in the crystal chemistry of aluminum fluc ride. The stable form of AlF_3 crystallize with a rhombohedral structure, space grou $R\bar{3}c$ (*1*), and transforms reversibly to th cubic ReO_3-type polymorph at 725 K (*1–3* We will refer to this rhombohedral form a the "α" form. A metastable form, calle β-AlF_3, was observed by several author (*4–7*); its structure is closely related to tha of hexagonal tungsten bronze (HTB), th distorsion leads to an orthorhombic cell wit b/a ratio extremely near to $\sqrt{3}$, generatin systematic twinning, in space group *Cmcr* (*7*). This β-form transforms slowly and irre versibly to the cubic polymorph. The trans formation takes place in a wide temperatur range (770–990 K), depending on the kineti conditions. This structure-type is als adopted by the β-forms of GaF_3 and InF

0022-4596/92 $5.0

(*7*), CrF_3 and VF_3 (*8*), and by $(H_2O)_{0.33}FeF_3$ (*9*). Another MX_3 corner-sharing octahedra tridimensional network is observed in the case of pyr-FeF_3 (*10*), obtained by "soft chemistry" from $(NH_4)_{0.5}FeF_3$ and crystallizing in the cubic pyrochlore structure-type; similar polymorphs were found for WO_3 (*11*) and $Al(OH,F)_3$ (*12*). This enumeration gives the full list of observed tridimensional MX_3 different networks exclusively built up from corner-sharing octahedra. Some others may be imaginated—but not necessarily found—by solid state chemists. The simplest derives from the tetragonal tungsten bronze (TTB) structure-type; various intergrowths built with the models quoted above can also be designed.

The t-AlF_3 structure presented here is quite different from the previously known MX_3 structure-types; moreover, to our knowledge, it was never predicted.

Experimental

We first encountered t-AlF_3 as a product of crystallization of an amorphous material, $AlF_3 \cdot xH_2O$ ($x < 0.5$), itself synthesized by dehydration under high-vacuum of $AlF_3 \cdot 9H_2O$ (*13*). Unfortunately, in these conditions, t-AlF_3 always appeared with an admixture of β-AlF_3. The reaction was followed by neutron powder time-resolved thermodiffractometry on the D1B instrument at the Institut Laue-Langevin. The formation of β-AlF_3 was detected between 520 and 730 K during the slow dehydration process evidenced by the background level evolution of the neutron diffraction pattern (Fig. 1). The formation of t-AlF_3 seems to start at the dehydration end ($\approx$730 K), from the remaining anhydrous amorphous AlF_3. Both polymorphs (β- and t-AlF_3) transform irreversibly in the ReO_3-type cubic AlF_3 form; in the conditions of the neutron experiment, all the sample was cubic-AlF_3 near 990 K; however, the transitions clearly took place in a wide temperature range, starting at least 200 K lower. Trying to reproduce in laboratory these observations proved to be difficult: various preparations of the amorphous material leading to quite different proportions of t-AlF_3 which was even sometimes not detected. From these synthesis, we were unable to determine the structure, although the neutron experiment allowed us to get, by difference, a reasonably good diffraction pattern of t-AlF_3, taking advantage of its selective growth from the anhydrous amorphous AlF_3. However, the data resolution was too low to discriminate between the two propositions at the indexing stage (a cubic-I cell with $a \approx 14.4$ Å or a tetragonal primitive one with $a \approx 10.2$ Å and $c \approx 7.2$ Å). Attempts to use X-ray powder diffraction were no more successful because of the simultaneous presence of β- and t-AlF_3.

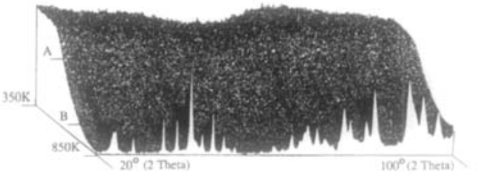

FIG. 1. Neutron time-resolved thermodiffractogram of the thermolysis of amorphous $AlF_3 \cdot xH_2O$. (A) and (B) indicate respectively the starting of the β- and t-AlF_3 formation. Wavelength: 2.51 Å.

A quasi-pure t-AlF_3 sample was obtained by dehydration under vacuum at 723 K of $[(CH_3)_4N]AlF_4 \cdot H_2O$ (*14*), following the global reaction:

$$[(CH_3)_4N]AlF_4 \cdot H_2O \rightarrow AlF_3 + H_2O + N(CH_3)_4F.$$

The chemical analysis confirmed the formulation (Al: 32.2%, calc. 32.1; F: 67.7%, calc. 67.8). It was not possible to avoid the presence of traces of α-AlF_3. The full study of thermal decomposition of $(TMA)M^{III}F_4 \cdot H_2O$ compounds of aluminum and iron by TG, DTG, DTA, and IR spectroscopy may be found in (*14b*).

TABLE I

CONDITIONS OF THE STRUCTURE DETERMINATION AND RIETVELD REFINEMENT FOR t-AlF$_3$

Space group		*P*4/*nmm*
Cell parameters (Å)	a =	10.1843(3)
	b =	7.1738(2)
Volume (Å^3)		744.07(5)
Z		16
2θ range (°)		10–140
Step scan (°2θ)		0.02
Time/step (sec)		30
Zones excluded (°2θ)		25.10 to 26.00
		57.78 to 59.00
Number of *hkl*		426
Number of refined parameters		
Total		65
x,y,z coordinates		15
Thermal parameters		37
Zeropoint (°2θ)		0.271(2)
Preferred orientation		
direction		001
parameter refined[a]		0.948(2)
Profile parameters		
	U_1 =	0.071(5)
(for a = 69, l = 140,	V_1 =	− 0.059(7)
see Eq. (1) in (*20*))	W_1 =	0.100(3)
	U_2 =	− 0.09(2)
	V_2 =	0.05(3)
	W_2 =	1.27(1)
	C =	− 0.043(1)
	D =	− 0.292(4)
Discrepancy factors[b]		
from pattern fitting	R_P =	0.067
	R_{WP} =	0.093
from Rietveld	R_B =	0.024
refinement	R_P =	0.070
	R_{WP} =	0.097
	R_E =	0.029

[a] March's model (*21*).

[b] R_P and R_{WP} are calculated after background subtraction and from "peak only."

Crystal Structure Determination and Refinement

As no single crystal was available, the structure determination was attempted from X-ray powder diffraction data. The powder pattern was recorded at 295 K on a Siemens D501 diffractometer (Cu$K\alpha$; graphite diffracted-beam monochromator). The same probable tetragonal cell was obtained using various automatic-indexing programs (as an example, the figures of merit obtained from the TREOR program (*15*) were $M(20)$ = 46 and $F(20)$ = 56.(0.0074, 49)). The ambiguity between the previous cubic and tetragonal propositions was easily suppressed in spite of a ratio a/c = 1.420. From the observed reflection conditions, the space groups *P*4/*nmm* or *P*4/*n* were selected. A clear line broadening characterized the reflections of the α-AlF$_3$ impurity, allowing the conclusion that it was affected by strong size and/or microstrain effects. The main contributions of the impurity to the powder pattern were eliminated by excluding two zones including the 304 reflection of t-AlF$_3$. Individual intensities were extracted from the powder pattern by using a local cell-constrained whole pattern fitting program. The main originality of this program is that the individual $|F_{obs}|$ are not refined in a least-squares sense, they are estimated from an iterative procedure based on the very simple principle which gives the so called "$|F_{obs}|$" in all Rietveld-type refinement programs (*16*). The SHELXS program was used for structure solution (*17*). Scattering factors and anomalous dispersion terms were taken from the "International Tables for X-ray Crystallography" (*18*). The direct methods were particularly designed for such a case where Al^{3+} and F$^-$ are isoelectronic. Trying first the *P*4/*nmm* space group, all the 11 independent atomic sites were obtained from the whole data set (426 reflections) as wel as from a reduced one (296 reflections eliminating those having a neighboring-one at less than 0.04°2θ). By using the SHELX76 program (*19*), the minimum R-factors obtained from the refinement o

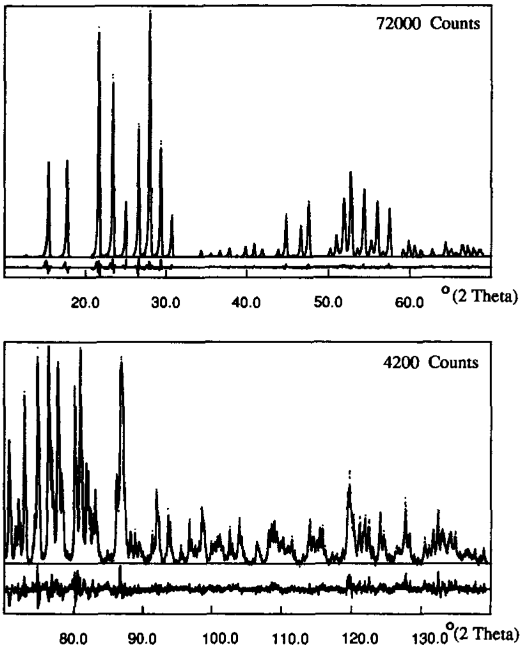

FIG. 2. Observed (· · ·) and calculated (———) X-ray powder pattern of t-AlF$_3$. The difference pattern is at the same scale.

the atomic coordinates and two isotropic thermal factors (one for the aluminum atoms and the other for the fluorine atoms) were $R = 0.21$ for the whole data set and $R = 0.16$ for the reduced one.

The final refinements were made by using a Rietveld program adapted to X-ray (*20*). With isotropic B-factors, the reliabilities were $R_B = 0.028$, $R_P = 0.072$, and $R_{WP} = 0.100$. All atom-types being light, the refinement of anisotropic thermal parameters was found possible and the result seemed reasonable. The conventional Rietveld reliabilities (background subtracted, peak-only) dropped to the final values presented Table I, which summarizes the conditions for the structure determination. Tests in the $P4/n$ space group did not improve the results. The agreement between the observed and calculated patterns is shown Fig. 2. Table II presents the atomic coordinates and thermal parameters; selected interatomic distances and angles are shown Table III.

Description of the Structure and Discussion

Figure 3 shows the projection of the structure of t-AlF$_3$ on (001). The 16 [AlF$_6$] octahedra of the unit cell may be distinguished on this figure; the tridimensional network of octahedra sharing only corners is, however, not immediately accessible. The structure can be described in terms of cross-linked chains of octahedra sharing *trans*-vertices. The chains, almost linear, are directed in several directions, one in the [001] direction, the others lying in planes parallel to the *ab*-plane, at three distinct levels along the *c*-axis. Figure 4 shows the cross-linked linear chains formed by the octahedra centered by Al(1) and Al(4) at the $z \approx 0$ level; these chains are directed toward the [110] and $[1\bar{1}0]$ directions, and they almost define a plane with [Al$_3$F$_{14}$] formulation, which is found as an isolated layer in the chiolite Na$_5$Al$_3$F$_{14}$ (*22, 23*). Figure 5 presents the cross-linked linear chains formed by the octahedra centered by Al(2) and Al(3). This time the chains are directed toward the [100] and [010] directions, at $z \approx \frac{1}{3}$ and $z \approx \frac{2}{3}$. They are related by an inversion center. The interconnection of such inverted chains produces two tetrahedral groups of corner-sharing octahedra (having only Al(2) at their center) as in the pyrochlore structure-type. Finally, the chains which are directed along the *c*-axis are formed by the Al(3) and Al(4)-centered octahedra; they are perfectly linear. One can note that most of the chains described above show octahedra alternating by a 45° rotation along the chain axis; the exception corresponds to the chains presenting two successive identically orientated octahedra belonging to the tetrahedral groups.

In this structure, all octahedra may be considered as quasi-regular, Al–F distances

TABLE II

ATOMIC COORDINATES AND THERMAL PARAMETERS FOR t-AlF$_3$

Atom	Site	x	y	z	B_{eq}
Al(1)	4*d*	0	0	0	1.12(8)
Al(2)	8*i*	$\frac{1}{4}$	0.9135(2)	0.3287(3)	1.37(8)
Al(3)	2*c*	$\frac{1}{4}$	$\frac{1}{4}$	0.4121(4)	1.08(13)
Al(4)	2*c*	$\frac{1}{4}$	$\frac{1}{4}$	0.9082(4)	0.79(10)
F(1)	16*k*	0.6216(2)	0.0524(2)	0.8390(3)	1.34(11)
F(2)	8*i*	$\frac{1}{4}$	0.0781(3)	0.4105(4)	2.02(17)
F(3)	8*j*	0.1215(2)	0.1215(2)	0.9089(3)	1.45(13)
F(4)	8*h*	0.1267(2)	−0.1267(2)	$\frac{1}{2}$	1.70(14)
F(5)	4*f*	$\frac{3}{4}$	$\frac{1}{4}$	0.2442(7)	1.19(23)
F(6)	2*c*	$\frac{1}{4}$	$\frac{1}{4}$	0.6633(7)	1.38(21)
F(7)	2*c*	$\frac{1}{4}$	$\frac{1}{4}$	0.1606(8)	1.61(21)

	U_{11}	U_{22}	U_{33}	U_{23}	U_{13}	U_{12}
Al(1)	131(9)	131(9)	163(15)	−8(8)	−8(8)	43(15)
Al(2)	159(10)	184(12)	178(10)	29(10)	0	0
Al(3)	137(15)	137(15)	138(20)	0	0	0
Al(4)	124(11)	124(11)	51(17)	0	0	0
F(1)	182(15)	174(14)	154(12)	44(11)	−1(11)	20(10)
F(2)	315(21)	275(23)	176(20)	−6(18)	0	0
F(3)	205(14)	205(14)	143(19)	27(10)	27(10)	−6(14)
F(4)	261(18)	261(18)	124(18)	14(10)	14(10)	−69(18)
F(5)	83(30)	184(32)	186(24)	0	0	0
F(6)	112(23)	112(23)	301(33)	0	0	0
F(7)	142(23)	142(23)	327(36)	0	0	0

Note. The U_{ij} vibrational coefficients relate to the expression: $T = \exp[-2\pi^2(h^2a^{*2}U_{11} + k^2b^{*2}U_{22} + l^2c^{*2}U_{33} + 2hka^*b^*U_{12} + 2hla^*c^*U_{13} + 2klb^*c^*U_{23})]$. (Uij are $\times 10^4$).

(see Table III) deviate little from the mean, which is well consistent with Shannon's ionic radii (*24*). The F–F distances are all in a very narrow range (2.47–2.62 Å), each F atom having eight F and two Al neighboring atoms. The Al–F–Al angles (140–180°) lie well within theoretical limits for stability (132–180°) (*25*)). A comparison between crystallographic features of the AlX_3 (X = OH,F) polymorphs at room temperature is shown Table IV. The density of t-AlF$_3$ is intermediate between those of α-AlF$_3$ and β-AlF$_3$. It may be recalled that t-AlF$_3$ exhibits a rather wide-temperature-range stability domain since it directly transforms into the ReO$_3$-type cubic polymorph. Owing to the differences between the structures of t-AlF$_3$ and the perovskite-type, the transformation is clearly reconstructive. According to the structure of the precursor [(CH$_3$)$_4$N]AlF$_4$ · H$_2$O (*14*), characterized by isolated dimeric entities of octahedra linked by edges, its transformation into t-AlF$_3$ appears to be also a fully reconstructive process.

Na$_4$Ca$_4$Al$_7$F$_{33}$ is the only material we have found to be related to t-AlF$_3$; its structure has been recently determined (*26*). In this structure, the [Ca$_4$Al$_7$F$_{33}$] part corresponds to an MX_3 3D network presenting a 3D six-connected net of Ca/Al atoms. Na$_4$ Ca$_4$Al$_7$F$_{33}$ and t-AlF$_3$ can be described as

TABLE III

Selected Interatomic Distances (Å) and Angles (°) for t-AlF_3

Al(1) Octahedron ⟨Al–F⟩ = 1.806

Al(1)	F(1)	F(1)	F(1)	F(1)	F(3)	F(3)
F(1)	**1.776(2)**	3.551(0)	2.506(2)	2.516(3)	2.531(2)	2.622(2)
F(1)	180.0	**1.776(2)**	2.516(3)	2.506(2)	2.622(2)	2.531(2)
F(1)	89.8(2)	90.2(2)	**1.776(2)**	3.551(2)	2.531(3)	2.622(2)
F(1)	90.2(2)	89.8(2)	180.0	**1.776(2)**	2.622(2)	2.531(3)
F(3)	88.0(2)	92.0(2)	88.0(2)	92.0(2)	**1.868(2)**	3.736(2)
F(3)	92.0(2)	88.0(2)	92.0(2)	88.0(2)	180.0	**1.868(2)**

Al(2) Octahedron ⟨Al–F⟩ = 1.796

Al(2)	F(5)	F(2)	F(4)	F(4)	F(1)	F(1)
F(5)	**1.772(3)**	3.548(3)	2.554(3)	2.554(3)	2.473(2)	2.473(2)
F(2)	179.3(3)	**1.776(3)**	2.518(3)	2.518(3)	2.585(3)	2.585(3)
F(4)	91.1(2)	89.4(3)	**1.804(3)**	2.511(2)	2.547(2)	3.614(2)
F(4)	91.1(2)	89.4(3)	88.2(2)	**1.804(3)**	3.614(2)	2.547(2)
F(1)	87.3(2)	92.2(3)	89.6(2)	177.3(2)	**1.811(3)**	2.615(2)
F(1)	87.3(2)	92.2(3)	177.3(2)	89.6(2)	92.5(2)	**1.811(3)**

Al(3) Octahedron ⟨Al–F⟩ = 1.768

Al(3)	F(2)	F(2)	F(2)	F(2)	F(6)	F(7)
F(2)	**1.751(3)**	2.476(3)	2.476(3)	3.501(5)	2.521(4)	2.506(5)
F(2)	90.0	**1.751(3)**	3.501(0)	2.476(3)	2.521(4)	2.506(4)
F(2)	90.0	179.2(0)	**1.751(3)**	2.476(3)	2.521(4)	2.506(4)
F(2)	179.2(4)	90.0	90.0	**1.751(3)**	2.521(4)	2.506(5)
F(6)	90.4(4)	90.4(3)	90.4(3)	90.4(4)	**1.802(5)**	3.606(7)
F(7)	89.6(4)	89.6(3)	89.6(3)	89.6(4)	180.0	**1.804(6)**

Al(4) Octahedron ⟨Al–F⟩ = 1.828

Al(4)	F(6)	F(7)	F(3)	F(3)	F(3)	F(3)
F(6)	**1.757(5)**	3.568(7)	2.555(4)	2.555(4)	2.555(4)	2.555(4)
F(7)	180.0	**1.811(6)**	2.586(4)	2.586(4)	2.586(4)	2.586(4)
F(3)	90.2(3)	89.8(4)	**1.851(3)**	3.702(3)	2.617(2)	2.617(2)
F(3)	90.2(3)	89.8(4)	179.7(3)	**1.851(3)**	2.617(2)	2.617(2)
F(3)	90.2(3)	89.8(4)	90.0	90.0	**1.851(3)**	3.702(3)
F(3)	90.2(3)	89.8(4)	90.0	90.0	179.7(3)	**1.851(3)**

Intercationic distances and Al–F–Al angles

Al(1)–Al(2)	3.580(1)	Al(1)–F(1)–Al(2)	173.6(2)
Al(2)–Al(3)	3.479(3)	Al(2)–F(2)–Al(3)	161.1(3)
Al(1)–Al(4)	3.660(1)	Al(1)–F(3)–Al(4)	159.7(2)
Al(2)–Al(2)	3.404(1)	Al(2)–F(4)–Al(2)	141.3(1)
Al(2)–Al(2)	3.330(1)	Al(2)–F(5)–Al(2)	140.0(1)
Al(3)–Al(4)	3.559(4)	Al(3)–F(6)–Al(4)	180.0
Al(3)–Al(4)	3.615(4)	Al(3)–F(7)–Al(4)	180.0

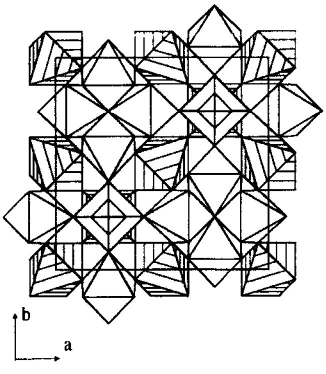

FIG. 3. Structure of t-AlF_3 projected onto (001). Al(1) at $z = 0$ are 3-shaded; Al(2) at $z \approx \frac{1}{3}$ and $\frac{2}{3}$ are unshaded; Al(3) at $z \approx \pm 0.4$ are 1-shaded; and Al(4) at $z \approx \pm 0.1$ are 5-shaded.

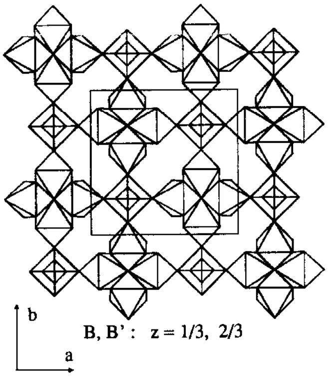

FIG. 5. Creation of tetrahedral groups of $[Al(2)F_6]$ octahedra by cross-linking of chains at $z \approx \frac{1}{3}$ (*B*) and $\frac{2}{3}$ (*B'*). Al(2) are unshaded and Al(3) are 1-shaded.

built from the same units but with a different stacking order. These units are the chiolite-type layer $[Al_3F_{14}]$ that we name "*A*" and the two cross-linked linear chains at z $\approx \frac{1}{3}$ in t-AlF_3, which would have a $[Al_5F_{24}]$ formulation, if they were isolated, and that we name "*B*." In this way, the t-AlF_3 structure is described by the *A–B–B'* stacking sequence along the *c*-axis (where (′) means translation and/or inversion); the $Na_4Ca_4Al_7F_{33}$ structure presents the *A–B–A'–B'* sequence in any *a,b,* or *c* directions since the structure is cubic (the formulation of the *A* sequence being $[Ca_2AlF_{14}]$ in $Na_4Ca_4Al_7F_{33}$). The full *A–B–A'–B'* sequence is represented Fig. 6. In $Na_4Ca_4Al_7F_{33}$, the sodium atoms are inserted in a cage which exists also in t-AlF_3, located between two tetrahedra of octahedra along the *c*-axis. This distances between the cage gravity-center and the Al atoms are

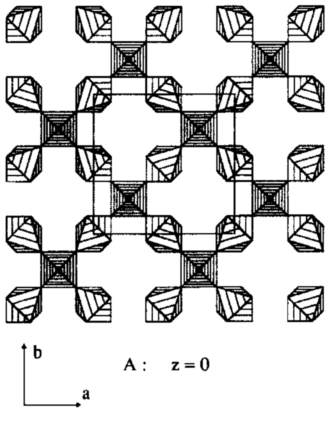

FIG. 4. The chiolite-type $[Al_3F_{14}]$ layer in t-AlF_3 at $z \approx 0$ (*A*). Al(1) are 3-shaded and Al(4) are 5-shaded.

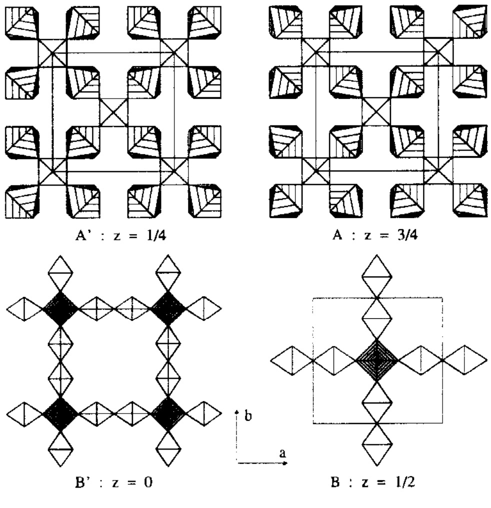

FIG. 6. The *A–B–A'–B'* sequence building $Na_4Ca_4Al_7F_{33}$. $[CaF_6]$ octahedra are 3-shaded, $[Al(1)F_6]$ octahedra are 5-shaded, and $[Al(2)F_6]$ are unshaded.

TABLE IV

CRYSTALLOGRAPHIC FEATURES OF AlX_3 POLYMORPHS

	Space group	a(Å)	b(Å)	c(Å)	Z	V/Z(Å^3)	Ref.
α-AlF_3	$R\bar{3}c$	4.9305(6)	4.9305(6)	12.4462(7)	6	43.67	(*1*)
t-AlF_3	$P4/nmm$	10.1843(3)	10.1843(3)	7.1738(2)	16	46.50	This work
β-AlF_3	$Cmcm$	6.931(3)	12.002(6)	7.134(2)	12	49.45	(*7*)
Al(OH,F)$_3$	$Fd3m$	9.7490(6)	9.7490(6)	9.7490(6)	16	57.91	(*12*)

within 2.88 and 3.60 Å. The size of this cage is greater in $Na_4Ca_4Al_7F_{33}$ with an environment of four Al atoms at 3.26 Å and four Ca atoms at 3.81 Å.

Some problems were encountered for the structure determination of $Na_4Ca_4Al_7F_{33}$, such as $\frac{2}{3}$ occupancy for the Na atoms and abnormally high anisotropic thermal motions for some fluorine atoms. It was concluded that only a mean structure had been described (*26*). It may be suggested that the local symmetry could be tetragonal and that the apparent cubic symmetry would be the consequence of microtwinning occurring because of easy faulting in the *A* and *B* building units sequence. From the *A* and *B* stacking building units point of view, the t-AlF_3 and $Na_4Ca_4Al_7F_{33}$ structures may be considered as polytypic, the latter being stuffed; thus other polytypes could be imaginated.

The existence of t-AlF_3 opens new fundamental research directions. One of the possible challenges would be to synthesize the hypothetical t-MF_3 (M = Fe, Cr, V, Ga, . . .), which would be quite interesting objects for physicists, particularly for the magnetic properties of some of them. Their existence does not seem unrealistic from a crystal chemistry point of view. Unfortunately, we have not been able to obtain t-FeF_3 from $[(CH_3)_4N]FeF_4 \cdot H_2O$.

Acknowledgment

The authors are indebted to the Institut Laue Langevin (Grenoble) for neutron facilities.

References

1. P. Daniel, A. Bulou, M. Rousseau, J. Nouet, J. L. Fourquet, M. Leblanc, and R. Burriel, *J. Phys.: Condens. Matter* **2,** 5663 (1990).
2. J. Ravez and A. Mogus-Milankovic, *Jpn. J. Appl. Phys.* **24-2,** 687 (1985).
3. J. Ravez and A. Mogus-Milankovic, *Mater. Res. Bull.* **19,** 311 (1984).
4. F. J. Christoph, Jr., M. D. Elkton, G. Teufer, and Ch. Ford, U.S. Patent 3, 178, 483, April 13 (1965).
5. A. Baumer, R. Caruba, and G. Turco, *C.R. Acad. Sci. Ser. D* **271,** 1 (1970).
6. D. B. Shinn, D. S. Crockett, and H. M. Haendler, *Inorg. Chem.* **5** (11), 1927 (1966).
7. A. Le Bail, C. Jacoboni, M. Leblanc, R. De Pape, H. Duroy, and J. L. Fourquet, *J. Solid State Chem.* **77,** 96 (1988).
8. R. De Pape, A. Le Bail, F. Lubin, and G. Ferey, *Rev. Chim. Miner.* **24,** 1 (1987).
9. M. Leblanc, G. Ferey, R. Chevallier, Y. Calage, and R. De Pape, *J. Solid State Chem.* **47,** 53 (1983).
10. R. De Pape and G. Ferey, *Mater. Res. Bull.* **21,** 971 (1986).
11. R. Nedjar, M. M. Borel, M. Hervieu, and B. Raveau, *Mater. Res. Bull.* **23,** 91 (1988).
12. J. L. Fourquet, M. Riviere, A. Le Bail, M. Nygrens, and J. Grins, *Eur. J. Solid State Inorg. Chem.* **25,** 535 (1988).
13. J. L. Fourquet and A. Le Bail, ILL Report, Experiment 5.22.313, 150 (1987).
14. (a) U. Bentrup and W. Massa, *Z. Naturforsch* **46b,** 395 (1991); (b) U. Bentrup, submitted for publication.
15. P. E. Werner, Z. Eriksson, and M. J. Westdahl, *J. Appl. Crystallogr.* **18,** 367 (1985).
16. A. Le Bail, unpublished ARITB program.
17. G. M. Sheldrick, *in* "Crystallographic Computing 3: Data Collection, Structure Determination, Proteins and Databases" (G. M. Sheldrick, C.

Kruger and R. Goddard, Eds.), p. 184, Clarendon, Oxford (1985).

18. "International Tables for X-ray Crystallography," Vol. IV, Kynoch Press, Birmingham (1974).
19. G. M. SHELDRICK, "SHELX-76, A program for crystal structure determination," Univ. of Cambridge (1976).
20. A. LE BAIL, H. DUROY, AND J. L. FOURQUET, *Mater. Res. Bull.* **23,** 447 (1988).
21. A. MARCH, *Z. Kristallogr.* **81,** 285 (1932).
22. C. BROSSET, *Z. Anorg. Allg. Chem.* **238,** 201 (1938).
23. C. JACOBONI, A. LEBLE, AND J. J. ROUSSEAU, *J. Solid State Chem.* **36,** 297 (1981).
24. R. D. SHANNON, *Acta Crystallogr., Sect. A***32,** 751 (1976).
25. A. F. WELLS, *J. Solid State Chem.* **6,** 469 (1973).
26. A. HEMON AND G. COURBION, *J. Solid State Chem.* **84,** 153 (1990).